Supporting Information

Cryo-synthesized Prussian Blue Analogues as Advanced Cathode Materials for Potassium-ion Batteries

Zhongli Qu[1,#], *Wendi Luo*[1,#], *Caitian Gao*[1,2,*], *Yanfang Liu*[3], *Zude Shi*[3], *Apparao M. Rao*[4], *Feifan Li*[1] & *Bingan Lu*[1,5,*]

[1]*School of Physics and Electronics, Hunan University, Changsha 410082, P. R. China;*

[2]*Greater Bay Area Institute for Innovation, Hunan University, Guangzhou, Guangdong Province 511300, P.R. China;*

[3]*College of Chemistry and Chemical Engineering, Hunan University, Changsha 410082, P. R. China;*

[4]*Department of Physics and Astronomy, Clemson Nanomaterials Institute, Clemson University, Clemson, South Carolina 29634, United States;*

[5]*State Key Laboratory of Advanced Design and Manufacturing for Vehicle Body, Hunan University, Changsha 410082, China*

#Contributed equally to this work.

*Corresponding authors (emails: Caitian Gao (ctgao@hnu.edu.cn), Bingan Lu (luba2012@hnu.edu.cn))

Experimental Section

Materials preparation:

The MnFe_PBA materials were prepared using the cryo-synthesis method.

MnFe_PBA_RT w/o EG: About 5 mmol potassium ferrocyanide trihydrate ($K_4Fe(CN)_6 \cdot 3H_2O$) was added to 50 ml of deionized water. Then, 5 mmol of manganese (II) sulfate monohydrate ($MnSO_4 \cdot H_2O$) and 5 mmol of potassium citrate were dissolved in 50 ml of deionized water. Next, the $MnSO_4$ and the $K_4Fe(CN)_6$ solutions were slowly added to the 50 ml of deionized water and stirred at room temperature. After stirring, the mixed solution was aged for 24 hours at room temperature. A white precipitate was obtained by centrifugation, which was cleaned thrice with deionized water and alcohol to remove impurities. Finally, the cathode material needed for the experiments was obtained by vacuum drying at 80 ℃.

MnFe_PBA_RT w EG: About 5 mmol potassium ferrocyanide trihydrate ($K_4Fe(CN)_6 \cdot 3H_2O$) was added to 50 ml of deionized water and 10 ml of EG. Then, 5 mmol of manganese (II) sulfate monohydrate ($MnSO_4 \cdot H_2O$) and 5 mmol of potassium citrate were dissolved in 50 ml of deionized water and 10 ml of EG. Next, the $MnSO_4$ solution and the $K_4Fe(CN)_6$ solution were slowly added to the 50 ml of deionized water and 10 ml of EG with stirring at room temperature. After stirring, the mixed solution was aged 24 hours at room temperature. A white precipitate was obtained by centrifugation, which was cleaned thrice with deionized water and alcohol to remove impurities. Finally, the cathode material needed for the experiment was obtained by vacuum drying at 80 ℃.

MnFe_PBA_Cryo_−10℃: The solutions were prepared as in MnFe_PBA_RT w EG's, but the prepared solutions were kept at −10 ℃ for 4 h. Next, the $MnSO_4$ solution and the $K_4Fe(CN)_6$ solution were slowly added to 50 ml of deionized water and 10 ml of EG with stirring at −10℃. After stirring, the mixed solution was aged 24 hours at room temperature. A white precipitate

was obtained by centrifugation, which was cleaned thrice with deionized water and alcohol to remove impurities. Finally, the cathode material needed for the experiment was obtained by vacuum drying at 80 ℃.

The 3,4,9,10-Perylenetetracarboxylic diimide (PTCDI) material was purchased from Sigma-Aldrich.

Electrode preparation:

The cathode slurry was prepared by mixing the active materials with Super P and polyvinylidene difluoride (PVDF) in N-Methylpyrrolidone (NMP) at a mass ratio of 7:2:1. Then the slurry was coated on carbon cloth and dried at 80 ℃ for 12 hours. The counter electrode slurry was prepared by mixing the activated carbon (AC) and PVDF in NMP at a weight ratio of 9:1. Then, the slurry was coated on a carbon cloth and dried at 80 ℃ for 12 hours. The anode slurry was prepared by mixing the PTCDI with Super P and PVDF in NMP at a mass ratio of 7:2:1. Then, the slurry was coated on carbon cloth and dried at 80 ℃ for 12 hours.

Electrolyte preparation:

21m KFSI in water was used as the electrolyte in all half and full cells.

Electrochemical measurements:

Three-electrode cells with Ag/AgCl electrode as reference electrode were assembled in air for electrochemical measurements. Two-electrode coin cells (CR-2032) with glass fiber (Whatman) as the separator were assembled in air for electrochemical measurements. The full battery was assembled in coin and pouch-cell formats. The full cells were assembled using a PTCDI anode, glass fiber separator, and PBA cathode, and the charge-discharge voltage range was 0-1.25 V at room temperature. These galvanostatic charge-discharge, CV, and GITT tests were performed on a multichannel battery testing system NEWARE (CT-4008) and Land (CT2001A (China).

EIS tests were carried out using electrochemical workstations (Admiral, Prime 1622, and Prime plus 1705). The EIS spectra of activation energy and *in situ* EIS spectra were collected in the 0.01 Hz-100000 Hz frequency range, and the corresponding resistances were obtained by fitting an equivalent circuit on the Zahner analysis application.

Materials characterization:

The SEM (Hitachi S-4800) and TEM (JEOL JEM-2100F) experiments were used to observe the morphology and the particle size distribution of MnFe_PBA_RT w/o EG, MnFe_PBA_RT w EG and MnFe_PBA_Cryo_−10℃. XPS (Kratos Axis Supra, take-off angle: 45^{o}) and XRD (Bruker D8 Advanced, Cu K_{α}) characterized the structural properties, crystallization degree, and phase compositions.

COMSOLMultiphysics simulation:

The COMSOL Multiphysics 5.6 Finite Element Simulation was used to simulate concentration distribution. These particles were generated using the MATLAB program, and the images generated by MATLAB were recognized by COMSOL and imported into geometry to form the entire computing domain. Calculated using the COMSOL Multiphysics 5.6 Finite Element Simulation, the current module in the built-in AC/DC module of COMSOL is used for calculation concentration on the boundary, the boundary flow, and the rest of the boundary is no flux boundary. The rate of diffusion is displayed by using concentration difference. The model size is selected as 1100×1100 nm.

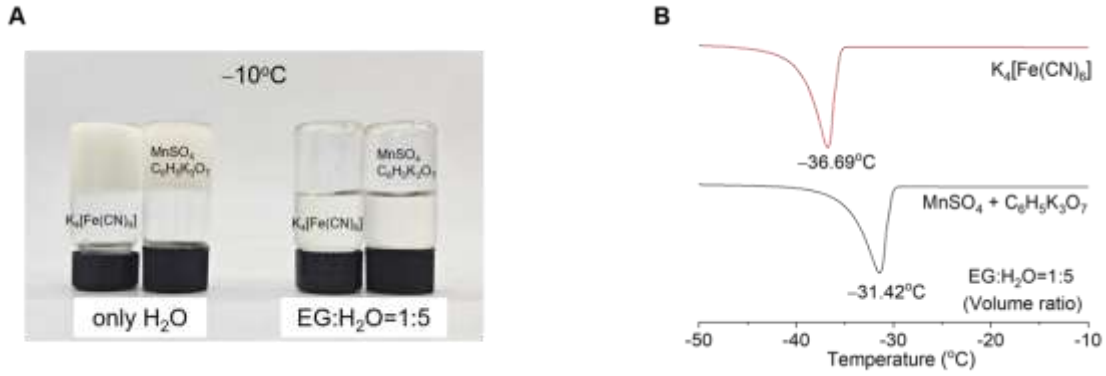

Figure S1 (A) Photographs of solutions with only water as a solvent (left) and addition EG (right). (B) DSC measurement for solutions with added EG (EG:H_2O=1:5 volume ratio) as a solvent.

For testing at a low temperature of −10°C, the solution with the addition of EG (EG:H_2O=1:5 volume ratio) still remained liquid. DSC measurement shows the freezing point of the solution with added EG is lower than −10 ℃, indicating that the improved solution can work properly at −10 ℃.

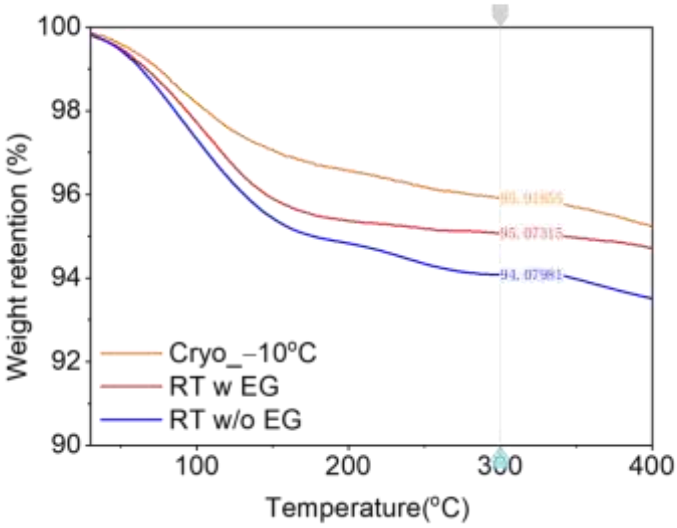

Figure S2 Thermogravimetric analysis (TGA) for the three materials used in this study. (MnFe_PBA_Cryo_−10℃, MnFe_PBA_RT w EG and MnFe_PBA_RT w/o EG)

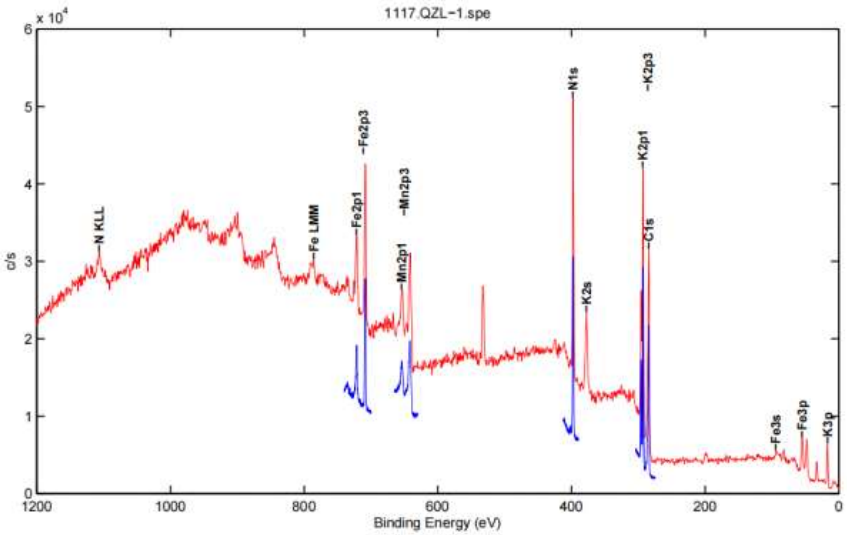

Figure S3 XPS analysis of the MnFe_PBA_Cryo_−10℃.

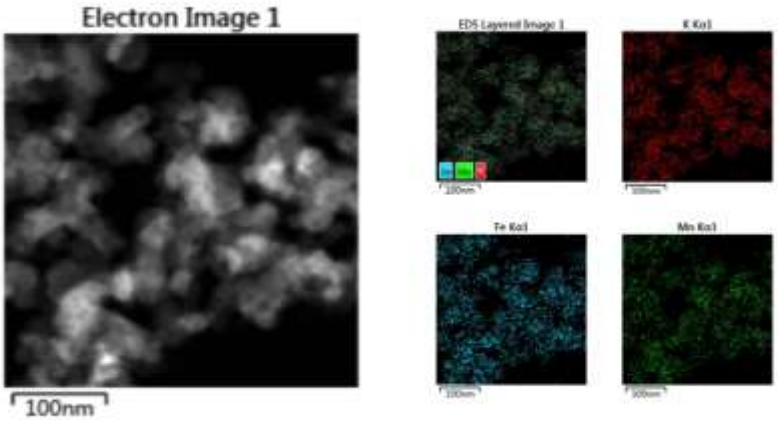

Figure S4 The TEM-energy dispersive spectroscopy (EDS) maps for elemental K, Fe, and Mn in MnFe_PBA_Cryo_−10℃.

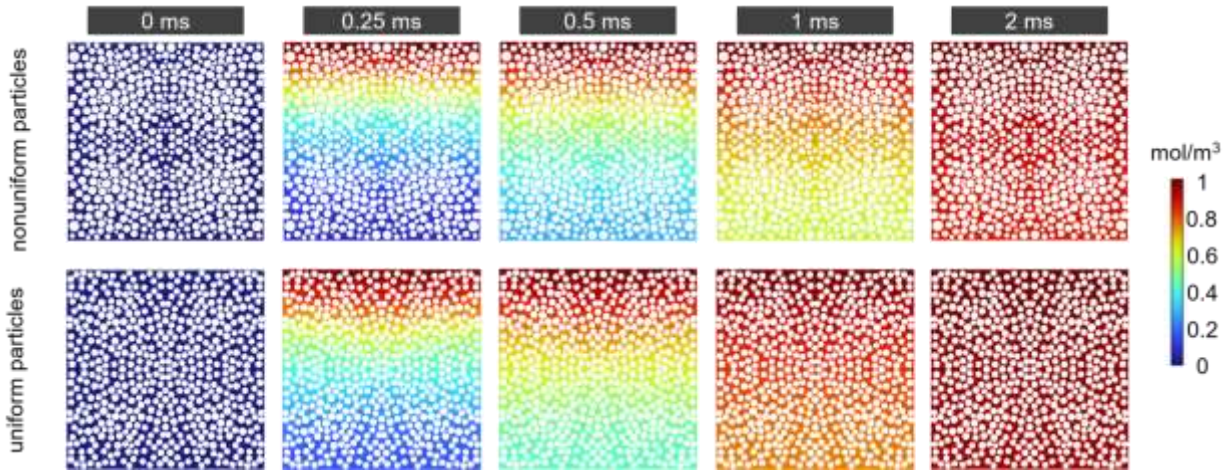

Figure S5 COMSOL simulations of the electrolyte concentration distribution at different moments (0 ms to 2 ms) for electrodes with nonuniform (upper) and uniform (lower) PBA particles.

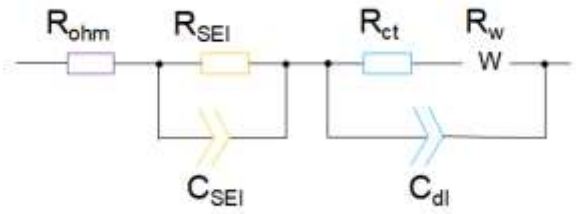

Figure S6 Equivalent circuit used to fit the impedance spectrum of the MnFe_PBA_Cryo_−10℃ || active carbon half cells.

Table S1 ICP-MS result of MnFe_PBA_Cryo_−10℃, MnFe_PBA_RT w EG and MnFe_PBA_RT w/o EG

	Cryo_−10℃	RT w EG	RT w/o EG
Weight of sample	0.0702 g	0.8048 g	0.0898 g
Content of K element	18.37%	19.45%	19.90%
Content of Fe element	13.70%	14.00%	14.43%
Content of Mn element	15.18%	14.81%	15.70%

Table S2 Performance comparison of aqueous batteries using PBAs as cathode

Materials	Specific capacity (mAh g^{-1}) / current (mA g^{-1})	Capacity retention (%) / cycle number	ref
MnFe_PBA_Cryo_−10℃	103 / 500	88 / 3500	This work
$Fe_4[Fe(CN)_6]$ ·3.4H_2O	84.7 / 1 C	80.8 / 1000	1
1$K_2Fe[Fe(CN)_6]$ ·2H_2O	120 / 200	96 / 500	2
ZnHCF	69.7 / 300	81 / 100	3
$K_2Ni[Fe(CN)_6]$ ·1.2H_2O	77.4 / 400		4
CoHCF	90.4 / 20	70 / 1000	5
KMHCF	57 / 200	52.6 / 400	6
$Na_{1.6}Mn_{0.75}[Fe(CN)_6]$ ·1.57H_2O	137 / 25	72.3 / 2700	7
FNMCF	109.8 / 100	77.8 / 200	8
$Na_2CoFe(CN)_6$	150/	90/200	9
KFeHCF	66 / 25	61.1 / 250	10
$Na_{1.58}Fe[Fe(CN)_6]_{0.87}$ 2.38H_2O	123 /	64.9 / 3000	11
PB-S3	116 / 10	71 / 500	12
$Na_2NiFe(CN)_6$	100 / 1C	79/250	13
$Na_2Cu_{0.6}Ni_{0.4}[Fe(CN)_6]$	62.5 /0.5C	96/1000	14
CuHCF	100 / 300	80 /250	15
$K_{0.71}Cu[Fe(CN)_6]_{0.72}$ 3.7H_2O	54 / 60	96.3 / 100	16
$K_3Fe[II]FeIII_6$ 2H_2O	120 / 4C	85 / 500	17
PB-K//AC	69.6 / 500	66.7 / 2000	18
KPB@ppy@Cloth	125 / 100	89.5 / 500	19
CuNiHCF	65 / 50	91 / 2000	20

References

1 Xia M, Zhang X, Liu T *et al.* Commercially available Prussian blue get energetic in aqueous K-ion batteries. *Chem Eng J* 2020;**394**:124923.

2 Su D, McDonagh A, Qiao S *et al.* High‐Capacity Aqueous Potassium‐Ion Batteries for Large‐Scale Energy Storage. *Adv Mater* 2017;**29**:1604007.

3 Zhang L, Chen L, Zhou X *et al.* Towards High‐Voltage Aqueous Metal‐Ion Batteries Beyond 1.5 V: The Zinc/Zinc Hexacyanoferrate System. *Adv Energy Mater* 2015;**5**:1400930.

4 Ren W, Chen X, Zhao C. Ultrafast Aqueous Potassium‐Ion Batteries Cathode for Stable Intermittent Grid‐Scale Energy Storage. *Adv Energy Mater* 2018;**8**:1801413.

5 Zhu K, Li Z, Jin T *et al.* Low defects potassium cobalt hexacyanoferrate as a superior cathode for aqueous potassium ion batteries. *J Mater Chem A* 2020;**8**:21103–9.

6 Han J, Mariani A, Zhang H *et al.* Gelified acetate-based water-in-salt electrolyte stabilizing hexacyanoferrate cathode for aqueous potassium-ion batteries. *Energy Storage Mater* 2020;**30**:196–205.

7 Shang Y, Li X, Song J *et al.* Unconventional Mn Vacancies in Mn–Fe Prussian Blue Analogs: Suppressing Jahn-Teller Distortion for Ultrastable Sodium Storage. *Chem* 2020;**6**:1804–18.

8 Chen X, Hua C, Zhang K *et al.* Control of Gradient Concentration Prussian White Cathodes for High-Performance Potassium-Ion Batteries. *ACS Appl Mater Interfaces* 2023;**15**:47125–34.

9 Wu X, Sun M, Guo S *et al.* Vacancy‐Free Prussian Blue Nanocrystals with High Capacity and Superior Cyclability for Aqueous Sodium‐Ion Batteries. *ChemNanoMat* 2015;**1**:188–93.

10 Wang Z, Zhuo W, Li J *et al.* Regulation of ferric iron vacancy for Prussian blue analogue cathode to realize high-performance potassium ion storage. *Nano Energy* 2022;**98**:107243.

11 Peng J, Zhang W, Hu Z *et al.* Ice-Assisted Synthesis of Highly Crystallized Prussian Blue Analogues for All-Climate and Long-Calendar-Life Sodium Ion Batteries. *Nano Lett* 2022;**22**:1302–10.

12 Wang W, Gang Y, Hu Z *et al.* Reversible structural evolution of sodium-rich rhombohedral Prussian blue for sodium-ion batteries. *Nat Commun* 2020;**11**:980.

13 Wu X, Cao Y, Ai X *et al.* A low-cost and environmentally benign aqueous rechargeable sodium-ion battery based on $NaTi_2(PO_4)_3$–$Na_2NiFe(CN)_6$ intercalation chemistry. *Electrochem Commun* 2013;**31**:145–8.

14 Li W, Zhang F, Xiang X *et al.* Nickel‐Substituted Copper Hexacyanoferrate as a Superior Cathode for Aqueous Sodium‐Ion Batteries. *ChemElectroChem* 2018;**5**:350–4.

15 Wang B, Wang X, Liang C *et al.* An All‐Prussian‐Blue‐Based Aqueous Sodium‐Ion Battery. *ChemElectroChem* 2019;**6**:4848–53.

16 Trócoli R, La Mantia F. An Aqueous Zinc‐Ion Battery Based on Copper Hexacyanoferrate. *ChemSusChem* 2015;**8**:481–5.

17 Su D, McDonagh A, Qiao S *et al.* High‐Capacity Aqueous Potassium‐Ion Batteries for Large‐Scale Energy Storage. *Adv Mater* 2017;**29**:1604007.

18 Bi H, Wang X, Liu H *et al.* A Universal Approach to Aqueous Energy Storage via Ultralow‐Cost Electrolyte with Super‐Concentrated Sugar as Hydrogen‐Bond‐Regulated Solute. *Adv Mater* 2020;**32**:2000074.

19 Lu K, Zhang H, Gao S *et al.* High rate and stable symmetric potassium ion batteries fabricated with flexible electrodes and solid-state electrolytes. *Nanoscale* 2018;**10**:20754–60.

20 Wessells CD, McDowell MT, Peddada SV *et al.* Tunable Reaction Potentials in Open Framework Nanoparticle Battery Electrodes for Grid-Scale Energy Storage. *ACS Nano* 2012;**6**:1688–94.